[3] Logan, J. G., "Hydrodynamic analog of the classical field equations," Phys. Fluids 5, 868–869 (1962).
[4] Landau, L. and Lifshitz, E., *The Classical Theory of Fields* (Addison-Wesley Press Inc., Cambridge, Mass., 1951), pp. 114–117.
[5] Logan, J. G., "A further note on propagation of thermal disturbances in rarefied-gas flows," AIAA J. 1, 942–943 (1963).

Residual Tensile Strength of Cracked Structural Elements

GEORGE GERARD*
Allied Research Associates, Concord, Mass.

Nomenclature

a = finite width correction factor
d = ligament width, in.
e = ductility ratio
k_e = elastic stress-concentration factor
k_p = plastic stress-concentration factor
k_s = stress-concentration strengthening factor
k_∞ = elastic stress-concentration factor for infinite width
L = notch length, in.
r = notch or crack radius, in.
w = width, in.
σ_{tu} = ultimate tensile strength, ksi
σ_{ty} = tensile yield strength, ksi

Introduction

AN analytical procedure for predicting the effects of determinate stress-concentration factors upon the strength of structural elements has been presented in Ref. 1. This method is based upon the reference value of the elastic stress-concentration factor in the structural element (which generally depends upon the local radius of curvature) and a characteristic of the material called the ductility ratio.

The limiting case of a stress concentration in a structural element is a crack. Here, the stress-concentration factor is indeterminate since the local radius of curvature is some function of the microstructure of the material and cannot be evaluated readily. Since the residual tensile strength of a structure containing relatively small cracks is of vital interest in many aerospace vehicle applications, it is of considerable importance to devise phenomenological approaches to this problem.

In the following, a modified stress-concentration factor approach is presented for determining the residual strength of structural elements containing cracks of limited extent. The ductility ratio that characterizes the material in the presence of a stress concentration and the effective radius of the crack are evaluated as a single material parameter from the test data correlation scheme presented herein.

Stress Concentration Factor Approach

Elastic stress concentration factors

For an infinitely wide sheet containing a central slit normal to the applied tension, Inglis[2] derived the following relation for the elastic stress-concentration factor in terms of the radius at the end of the slit r and the slit half-length L (see Fig. 1):

$$k_\infty = 1 + 2\,(L/r)^{1/2} \tag{1}$$

In an extension of Inglis' result to strips of finite width, Dixon[3] derived the following correction factor:

$$a = \frac{k_e}{k_\infty} = \left(\frac{d/w}{2 - d/w}\right)^{1/2} \tag{2}$$

By combining Eqs. (1) and (2),

$$k_e = a\,[1 + 2\,(L/r)^{1/2}] \tag{3}$$

Both Eqs. (2) and (3) have been confirmed by photoelastic test results reported by Dixon[3] and Papirno.[4] For convenience, the finite width correction factor given by Eq. (2) is plotted in Fig. 1.

Plastic stress concentration factors

Equations (1–3) pertain to the elastic region of the stress-strain curve of a material. In the plastic region and at failure, it is necessary to consider the influence of plasticity upon the elastic stress-concentration factor. In Ref. 1, the following semi-empirical relationship between the plastic stress-concentration factor k_p and the elastic one was suggested:

$$k_p = (1/k_s) + [k_e - (1/k_s)]e \tag{4}$$

Here, e is the ductility ratio that is a characteristic of the material. The factor k_s accounts for the notch strengthening resulting from the multiaxial stress field existing in the vicinity of the notch.

By rearranging Eq. (4) in the following form,

$$k_p = (1/k_s)(1 - e) + k_e e \tag{5}$$

it is possible to evaluate both e and k_s from a series of strength tests on specimens containing determinate stress-concentration factors in which the net section stress is elastic. This procedure is illustrated in some detail in Refs. 1 and 5 and consists of plotting k_p vs k_e, which generally is linear. The ductility ratio then is evaluated from the slope and k_s from the intercept.

Now, by inserting Eq. (3) into Eq. (5), one obtains

$$k_p = (1/k_s)(1 - e) + ae + 2\,a\,L^{1/2}\,(e/r^{1/2}) \tag{6}$$

In cases where the slit length is held fixed and r is varied to achieve different determinate stress-concentration factors, then L, a, and k_s are fixed quantities. By plotting k_p vs $r^{1/2}$, when the net section stress is elastic, the ductility ratio can be evaluated from the slope of the straight line and k_s from the intercept. This procedure corresponds essentially to that used in connection with Eq. (5).

Indeterminate stress concentrations

When cracks are considered, however, the geometric conditions of the problem are somewhat different. Now, the radius at the root of the crack is essentially constant, although

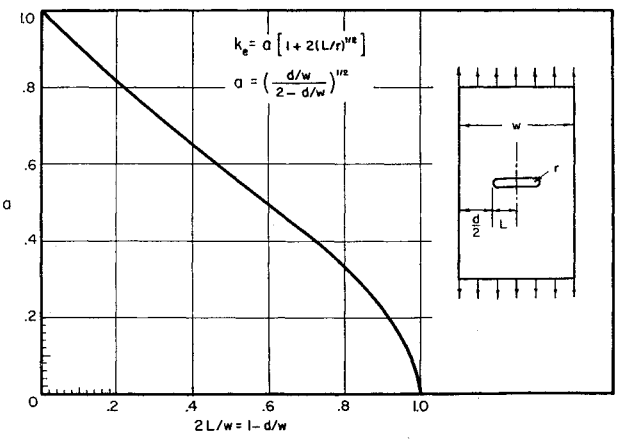

Fig. 1 Elastic stress concentration for an internally notched tension strip of finite width

Received by IAS November 29, 1962.
* Director of Engineering Sciences. Associate Fellow Member AIAA.

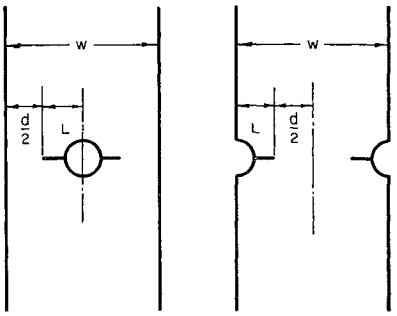

Fig. 2 Test specimen configurations

unknown. The independent variables are generally the crack length and specimen width, in which case L and a vary.

By plotting k_p vs $aL^{1/2}$, a linear relation should result when the net section stress is elastic. The slope of this line according to Eq. (6) is the quantity $e/r^{1/2}$, which can be interpreted as a material crack-ductility characteristic, since both e and r are associated with the microstructural properties of the material. Since L is variable, so are a and k_s, and it is not possible to interpret the intercept directly.

However, it can be noted that, in a structural application where the crack length may be very small relative to the pertinent structural dimensions, a and k_s both approach unity and Eq. (6) reduces to

$$k_p = 1 + 2L^{1/2}\,(e/r^{1/2}) \qquad (7)$$

Correlation of Crack Test Data

In most experiments on the residual strength of strips containing cracks, a determinate stress concentration such as a circular hole or notch is introduced first. The strip then is subject to axial fatigue loading to produce a crack of the desired length. The configurations of the test specimens are similar to those shown in Fig. 2.

The testing of tensile strips containing cracks has certain shortcomings that are difficult to overcome and must be recognized in the analysis of such data. As shown in Fig. 2, the crack length L includes the circular hole or notch used to initiate the crack. If the crack is of sufficient length, then the stress-concentration factor can be based on the crack length L, as shown photoelastically in Ref. 4. If the crack is too short, then the presence of the notch may modify the stress-concentration factor based on L, somewhat.

A second source of possible error is the fact that the two crack lengths generally are not identical, which introduces an unsymmetrical loading situation. This sometimes, but not always, is corrected by using a saw cut to lengthen the shorter crack. A third source of error arises when the crack becomes relatively long, and transverse buckling of the strip can occur in the region of the crack. When this occurs, the observed residual strength can be reduced seriously by the presence of the buckles, and supporting guide plates sometimes are used to minimize buckling.

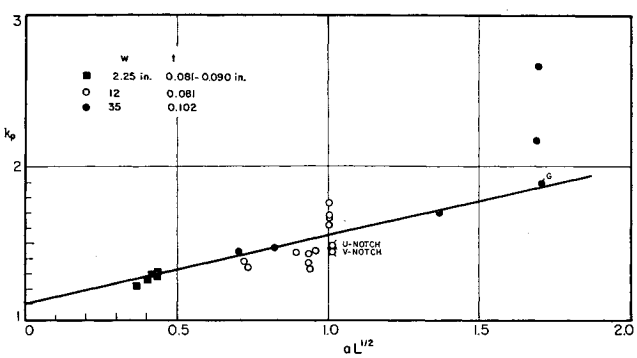

Fig. 3 Test data on 2024-T3 aluminum alloy sheet specimens

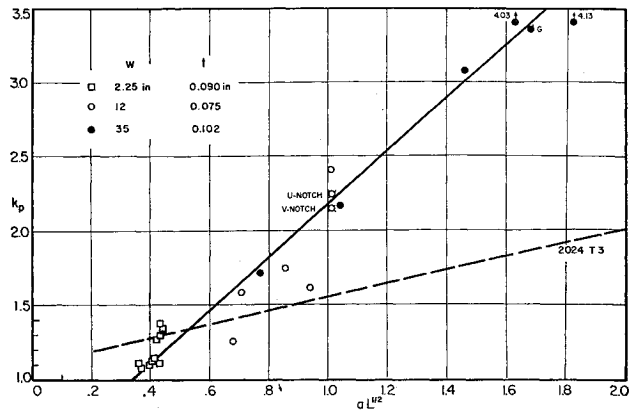

Fig. 4 Test data on 7075-T6 aluminum alloy sheet specimens

Analysis of test data

With these shortcomings in the background, some published test data are examined now in order to evaluate the correlation scheme suggested by Eq. (6). In all cases, the plastic stress-concentration factor k_p is based upon the area of the net section at the crack, and the crack length is measured in the manner shown in Fig. 2. The finite width correction factor a is determined from Fig. 1 for the pertinent crack geometry.

McEvily, Illg, and Hardrath[6] reported test results on a variety of 2024-T3 and 7075-T6 aluminum alloy sheet specimens containing fatigue cracks. Three different specimen widths were used: 2.25-in. wide with edge notches of 0.375-in. radius, and 12-in.- and 35-in.-wide sheets with 0.50-in. radius central holes. For the 2.25-in. specimens, the eccentricity was reduced by introducing a saw cut at the uncracked notch equal in length to the crack at the other notch. The wider specimens were tested generally with cracks emanating from both sides of the central hole, although no attempt was made to reduce the eccentricity that may have been present. In addition, the 35-in.-wide specimens with a total crack area of approximately 50% of the gross area were retested with supporting guides to minimize buckling effects.

In Fig. 3, the test data for the three 2024-T3 sheet specimen widths are shown in terms of the parameters of Eq. (6), where k_p is plotted as a function of $aL^{1/2}$. It can be observed that the data correlate reasonably well when the inherent difficulties in the test procedure are considered. At a value of $aL^{1/2} = 1.7$, the point marked G was tested using guides to reduce buckling. It is through this point that the straight line implied by Eq. (6) is drawn in Fig. 3.

Also shown in Fig. 3 are two test points at $aL^{1/2} = 1$ which correspond to the auxiliary tests reported in Ref. 6. These tests were conducted on specially prepared U and V notch specimens of 12-in. width containing 2-in.-deep notches terminating in a radius of 0.005 in. It can be observed that these data correlate reasonably well with the cracked specimen data.

In Fig. 4, corresponding test data are shown for the 7075-T6 sheet specimens. Again, within the shortcomings of the test procedure, the test data on the cracked and notch specimens correlate reasonably well with the straight line shown.

Also shown in Fig. 4 is the straight line for the 2024-T3 data taken from Fig. 3. It can be observed that a crossover point occurs at a value of $aL^{1/2}$ of approximately 0.5, which corresponds roughly to a $\frac{1}{4}$-in. crack in a structure. It is quite apparent that, on the basis of residual tensile strength considerations, 7075 T-6 aluminum alloy is superior to 2024-T3 aluminum alloy for small cracks (approximately less than $\frac{1}{4}$ in.). The reverse situation is true for larger cracks.

A similar situation is evident in Fig. 5, which is based on

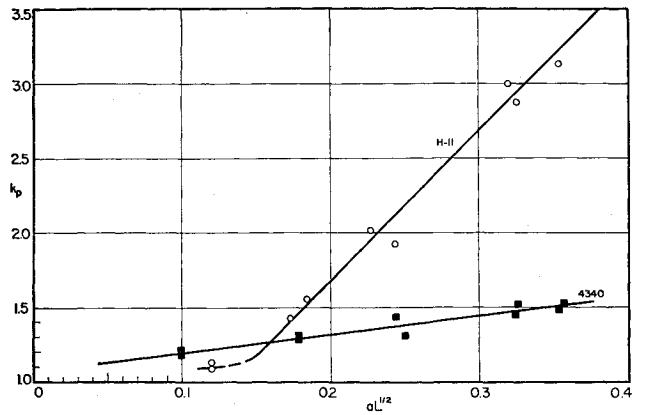

Fig. 5 Test data on 0.070-in.-thick sheet specimens of H-11 and 4340

Manning's data[7] on 4340 and H-11 steels. Both steels had the same yield strength of 225 ksi with an ultimate tensile strength of 260 ksi for 4340 and 270 ksi for H-11. The tests were conducted on specimens 1.5-in. wide with fatigue cracks emanating from a central circular hole that was varied in radius. It can be observed that the test data correlate reasonably well with the straight lines shown in Fig. 5.

In this case, the crossover point occurs at a value of $aL^{1/2} = 0.16$, which corresponds to a crack length of 0.025 in. ($\frac{1}{8}$ of the thickness) in a structure. The crossover point in both Figs. 4 and 5 appears to be associated with the effects of plasticity at the lower values of k_p. As discussed in relation to Eq. (6), a linear relation between k_e and k_p can be expected when the net section stress is elastic. At low values of k_p the net section stress is in the plastic range, and the departure from a straight line shown for the lowest H-11 data points in Fig. 5 is to be expected.

Equation (6) indicates that the slope of the straight line through the test data is a measure of the crack-ductility ratio $e/r^{1/2}$. The values shown in Table 1 were obtained from Figs. 3–5.

Conclusions

1) From the test data presented herein, it appears that the use of Eq. (6) is satisfactory for correlating test data on the residual strength of fatigue cracked specimens of varying widths.

2) This correlation scheme indicates that, although higher strength materials may be more notch sensitive for larger crack lengths, they also may be less sensitive for small crack lengths than lower strength materials. This phenomenon appears to be associated with the effects of plasticity.

References

[1] Gerard, G., "Structural significance of ductility in aerospace pressure vessels," ARS J. **32**, 1216–1221 (1962).

[2] Inglis, C. E., "Stresses in a plate due to the presence of cracks and sharp corners," Trans. Inst. Nav. Arch. **55**, Part 1 (1913).

[3] Dixon, I. R., "Stress distribution around a central crack in a plate loaded in tension; effect of finite width of plate," J. Roy. Aeronaut. Soc. **64**, 141–145 (1960).

[4] Papirno, R., "Stress concentrations in tensile strips with central notches of varying end radii," J. Roy. Aeronaut. Soc. **66**, 323–326 (1962).

Table 1 Summary of correlated test data

Material	σ_{tu}, ksi	σ_{ty}, ksi	$e/r^{1/2}$, in.$^{-1/2}$
2024-T3	72	53	0.23
7075-T6	80.5	74	0.89
4340	260	225	0.63
H-11	270	225	4.95

[5] Gerard, G. and Papirno, R., "Ductility ratio of aged beta titanium alloy," Am. Soc. Metals Trans. Quart. **55**, no. 3, 373–388 (1962).

[6] McEvily, A. J., Illg, W., and Hardrath, H. F., "Static strength of aluminum-alloy specimens containing fatigue cracks," NACA TN 3816 (October 1956).

[7] Manning, G. K., "How should you evaluate high-strength materials?" Metal Progr. **80**, no. 3, 65–67 (1961).

Shape of the Porous Two-Dimensional Hypersonic Sail

E. A. Boyd*
College of Aeronautics, Cranfield, England

In an earlier note[1] the author pointed out how one may calculate the effect of porosity on the characteristics of the two-dimensional supersonic sail.[2] (M. R. Fink, United Aircraft Corporation, has drawn the author's attention to a similar study of the impermeable supersonic sail he published in an internal company report.[3]) Here the effect of porosity on the shape is calculated, and hence the modification to the aerodynamic performance of the impermeable hypersonic sail studied by Daskin and Feldman[4] and by the author.[5]

First establish the loading on the porous sail in a Newtonian flow (see Fig. 1 for notation). A thin shock layer forms on the concave forward-facing surface of the sail. Define P such that $\rho_\infty U^2 P$ is the momentum flow in the shock layer per unit depth. Assume that the velocity along a streamline within the shock layer is constant. For a streamline entering the shock layer where the inclination is θ' this velocity is $U\cos\theta'$. Thus, since the differential element of mass flow per unit depth is $\rho_\infty U\,dy'$, the value of P at y is

$$P = \int_0^y \cos\theta'\,dy' \tag{1}$$

Because of the porosity there is a normal velocity v through the sail, where one may write

$$v/u = \sigma(p)(p/q_\infty) \tag{2}$$

Here p is the pressure difference across the sail, and σ is a parameter describing the porosity.

The drag of that part of the sail between $y = 0$ and y is calculated most easily from a momentum balance. The drag per unit depth

$$D = \rho_\infty U^2 y - \rho_\infty U^2 P\cos\theta - \rho_\infty U\int_0^y v\sin\theta'\,dy' \tag{3}$$

and the drag coefficient for unit chord

$$C_D = 2y - 2P\cos\theta - 2\int_0^y \frac{v}{U}\sin\theta'\,dy' \tag{4}$$

The pressure difference $p(y)$ across the sail is given by

$$p/q_\infty = dC_D/dy = 2\sin^2\theta + 2\sin\theta\frac{d\theta}{dy}\int_0^y \cos\theta'\,dy' - 2\sigma(p)\frac{p}{q_\infty}\sin\theta \tag{5}$$

$$(p/q_\infty)[1 + 2\sigma(p)\sin\theta] = 2\sin^2\theta + 2\sin\theta\frac{d\theta}{dy}\int_0^y \cos\theta'\,dy' \tag{6}$$

The shape of the sail is found by substituting this loading

Received by IAS December 11, 1961.

* Lecturer, Department of Aerodynamics.